JACS
JOURNAL OF THE AMERICAN CHEMICAL SOCIETY
Communication
pubs.acs.org/JACS

Kinetic Intermediates in Amyloid Assembly

Chen Liang,‡ Rong Ni,‡ Jillian E. Smith,‡ W. Seth Childers,† Anil K. Mehta,* and David G. Lynn*

Departments of Chemistry and Biology, Emory University, Atlanta, Georgia 30322, United States

Supporting Information

ABSTRACT: In contrast to an expected Ostwald-like ripening of amyloid assemblies, the nucleating core of the Dutch mutant of the Aβ peptide of Alzheimer's disease assembles through a series of conformational transitions. Structural characterization of the intermediate assemblies by isotope-edited IR and solid-state NMR reveals unexpected strand orientation intermediates and suggests new nucleation mechanisms in a progressive assembly pathway.

The self-assembly of proteins into amyloid is an initiating step in misfolding[1,2] and infectious prion[3] diseases. The process is traditionally described as a thermodynamically driven "ripening" of accessible conformations, and the range of phases that exist under a given set of conditions is the result of amyloid polymorphism. Recently, secondary nucleation sites[4,5] have suggested the possibility of a more progressive pathway contributing to different assembled phases. Here we experimentally demonstrate that the minimal nucleating core[6,7] of the Dutch mutant[8] of the Aβ peptide of Alzheimer's disease (AD), Aβ(16−22)E22Q or Ac-^{16}KLVFFA^{22}Q-NH_2, assembles as antiparallel β-strands that later transition completely into parallel β-strands. These studies define a progressive pathway for amyloid assembly, even for simple model peptides, and reveal new mechanisms for achieving polymorphic diversity in disease etiology.

Simulation[9−14] and empirical[15−22] analyses of Aβ(16−22) assembly are consistent with an initial solvation free-energy driven oligomerization to a particle phase. We reasoned that secondary structure formation within the less hydrated peptide particle phase[22−24] may explain the observation that Aβ(16−22)E22L, Ac-^{16}KLVFFA^{22}L-NH_2, matures with antiparallel strand orientations.[19] Electrostatic repulsion between lysine side chains would select against charged N-terminal lysine residue proximity in parallel strands (Figure 1) during nucleation.

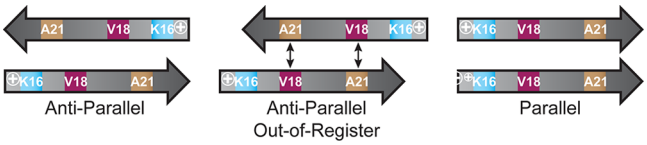

Figure 1. Strand conformations of Aβ(16−22)E22L peptide showing positions of charged lysine (blue) residues. Electrostatic repulsion is attenuated in antiparallel peptide orientation. Out-of-registry strands place the bulky valine packed with the less bulky alanine. Arrows indicate valine (red)-alanine (brown) cross-strand pairing.

Given that antiparallel out-of-register alignment in Aβ(16−22)E22L is directed by the preference of the bulky valine side chain at position 18 being across (cross-strand pairing) from the less bulky alanine,[19,20] we hypothesized that uncharged substitutions would stabilize different strand arrangements. Structural[25,26] and thermodynamic[27] investigations have identified ordered glutamine side chains in cross-strand stabilization of parallel registries, and the Dutch mutant of Aβ,[8] manifested as the Aβ(16−22)E22Q congener which conservatively swaps a side chain -OH for an -NH_2, appeared suitable to change the energy balance. Quite distinct from previous cytosine substitution[28] or metal ion binding elements which stabilize sheet stacking interactions,[29] the E22Q substitution could stabilize parallel strand registry through cross-strand pairing via amide side-chain H-bonding.

Figure 2A shows particles and short twisted ribbons that appear in electron micrographs early after Aβ(16−22)E22Q peptide dissolution, and the FT-IR amide-I stretch centered at 1625 ± 1 cm^{-1} indicates β-sheet assembly (Figure S1). In contrast with the design for glutamine addition, isotope-edited IR analysis with $^{13}C{=}O$ enrichment at the central F19 residue [1-^{13}C]F19Aβ(16−22)E22Q, where $^{12}C/^{13}C$ coupling is most diagnostic of β-strand registry,[19,30,31] shows a band splitting[19,31−34] of almost 40 cm^{-1} and a $^{12}C/^{13}C$ band intensity ratio of <1 (Figures 2C, black, S2). These assignments are consistent with previously characterized assemblies[30,31,33−37] and define one-residue out-of-register antiparallel stranded β-sheets (Figure 1).

However, these assemblies do not persist. Approximately 1 week after assembly is initiated the FT-IR spectra begin a cooperative transition into long smooth fibers that after 20 days have diameters of 11.6 ± 1.2 nm (Figures 2B, S3). Changes in the frequency and amplitude of the $^{12}C/^{13}C$ amide-I bands (Figures 2D, S4) track with the morphological transitions seen by EM. A CO stretch at 1677 cm^{-1} assigned to ordered glutamine side chains[38,39] grew with the transition. The final assemblies with circular dichroism ellipticity minimum at 217 nm (Figure S5) and X-ray powder diffraction (Figure S6) *d*-spacing reflections at 4.76 and 10.1 Å are typical of cross-β assemblies.[19]

The orientation and specific registry of each Aβ(16−22)E22Q strand is defined via the rate of double-quantum coherence build-up through homonuclear dipolar coupling in ^{13}C DQF-DRAWS[40] solid-state NMR experiments. Using the infinite array approximation[28,41,42] (Figure S7) and including the effects of double quantum relaxation,[41] T_2DQ = 11.7 ms

Received: August 21, 2014
Published: October 14, 2014

   dx.doi.org/10.1021/ja508621b | J. Am. Chem. Soc. 2014, 136, 15146−15149

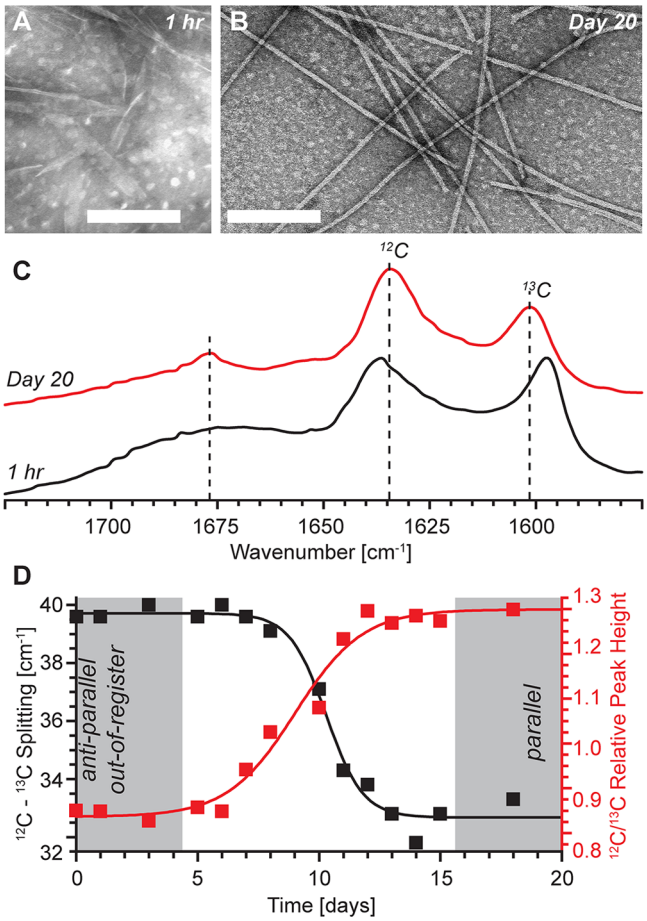

Figure 2. Time dependence of the assembly of 1 mM Aβ(16–22)E22Q at acidic pH in 20% CH_3CN containing 0.1% TFA monitored by TEM (A,B) and isotope-edited IR analysis (C,D) using [1-^{13}C]F19 Aβ(16–22)E22Q assemblies. (A) After 1 h, wide ribbons (up to 40 nm) are observed, in contrast to (B) the 11.6 ± 1.2 nm fibers present after 20 days. (C) Dashed lines indicate positions of glutamine side chain, ^{12}C and ^{13}C amide-I band positions in mature fibers. (D) ^{12}C/^{13}C splitting (black) and relative peak height (red) for assemblies collected at multiples of 24 h as indicated on the time axis. Scale bars are 200 nm.

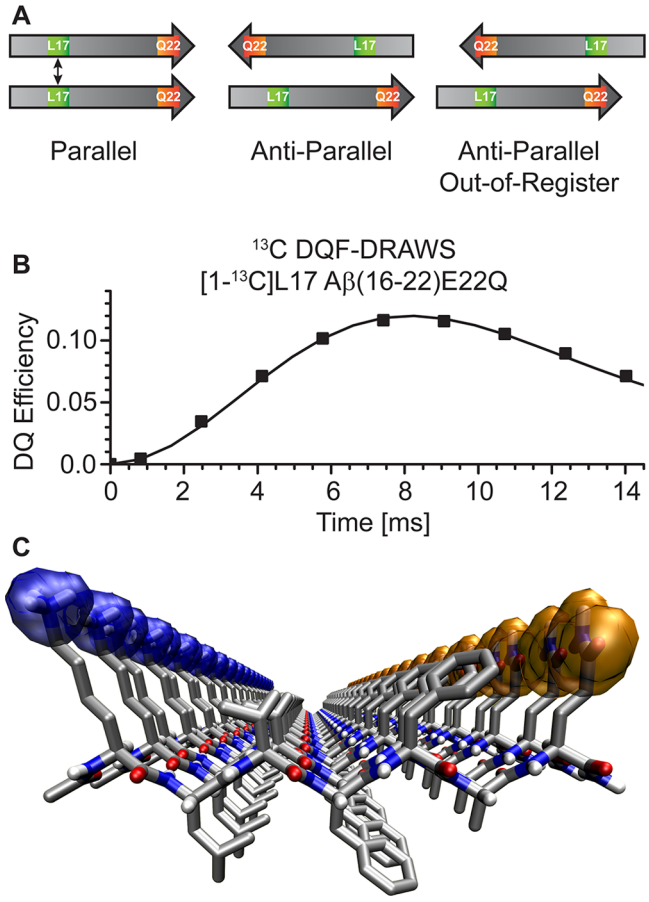

Figure 3. β-sheet registry in Aβ(16–22)E22Q assemblies. (A) Cartoons showing positions of ^{13}C enriched residues (green) in various β-sheet registries. (B) Determination of peptide registry with ^{13}C–^{13}C distance measurements between leucine backbone carbonyls of 1 mM [1-^{13}C]L17 Aβ(16–22)E22Q assembled as fibers with ^{13}C DQF-DRAWS NMR pulse sequence. Data points are peak intensity for double-quantum buildup divided by total ^{13}C signal intensity. Best fit to DQ buildup (black line) is with a 4.7 Å ^{13}C–^{13}C distance. (C) Aβ(16–22)E22Q parallel β-sheet registry. For clarity, nonpolar hydrogen atoms are not displayed, but the lysine (blue) and glutamine (gold) tracts are highlighted.

(Figure S8), the buildup of [1-^{13}C]-L17 intensity from enriched E22Q assemblies uniquely fits a parallel in-register strand arrangement (Figures 3B, S9). These analyses do not support the glutamine/intersheet H-bonding (Q-tracks) prevalent in Huntington's inserts,[26] as they require laminate spacings[43] of 8 Å for backbone to side chain H-bonding rather than the 10.1 Å spacing seen in these assemblies. These data, together with the glutamine side chain CO stretch at 1677 cm^{-1} (Figure 2C, red), are consistent with cross-strand pairing along the sheet surface through extended side chain H-bonding Q-tracks as shown in Figure 3C.[25,26]

H-bond pairing is indirectly evaluated with N^5-methylated, Aβ(16–22)E22QNHCH$_3$, and N^5,N^5-dimethylated, Aβ(16–22)E22QN(CH$_3$)$_2$, peptides. The N^5,N^5-dimethyl peptide (Figure S10C) assemblies, as visualized with EM, appear morphologically indistinguishable from Aβ(16–22) nanotubes and ribbons.[17,19,22] With [1-^{13}C]F19 enrichment, the ^{12}C/^{13}C band splitting is 40 cm^{-1}, and the diagnostic antiparallel band at ~1695 cm^{-1} (Table S1 and Figure S10D) supports the same one-residue out-of-register antiparallel β-strands. Unlike Aβ(16–22)E22Q, no distinct IR band at 1677 cm^{-1} diagnostic for ordered glutamine side chains is apparent in the N^5,N^5-dimethylated glutamine peptide assemblies. In contrast, the monomethylated Aβ(16–22)E22QNHCH$_3$ peptide assembles as fibril bundles (Figure S10B) with individual widths ranging from 7 nm in a single fiber to bundles containing up to five twisted fibers (Figure S11). Time-dependent IR spectra of assembling [1-^{13}C]F19 enriched monomethyl peptides (Figure S12) reveal a similar early antiparallel orientation that also transitions to parallel with growth of the glutamine side chain band at 1677 cm^{-1}, but the spectra are most consistent with the mature assemblies containing a mixture of parallel, antiparallel in-register, and antiparallel out-of-register assemblies (Figure S12, inset). Monomethylation appears to weaken the extended glutamine side chain H-bonding Q-track and is expected to create a methylated surface. We predict that mixed fibers, or even mixed domains within individual fibers, are responsible for the bundling.

These data argue that the nucleating core of the Aβ peptide of AD follows an obligatory hydrophobic collapse to intermolecular molten particles.[22−24] The E22Q substitution

dx.doi.org/10.1021/ja508621b | J. Am. Chem. Soc. 2014, 136, 15146−15149

provides an energetic constraint sufficient for a new transition and one that does not manifest in the molten particle phase. The addition of 1% by weight preassembled fibers prepared from mature parallel E22Q assemblies completes the transition to parallel strands within hours (Figure 4, S13). Once initiated, parallel strand assembly propagates quickly, establishing the propagation of parallel strands is not limiting.

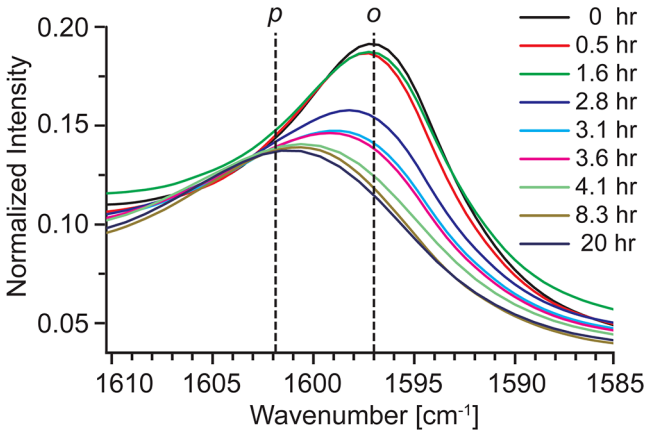

Figure 4. Time dependence of Aβ(16−22)E22Q assembly upon seeding with 1% preformed Aβ(16−22)E22Q fibers. FT-IR spectra of ^{13}C amide-I band of 0.8 mM [1-^{13}C]F19 Aβ(16−22)E22Q seeded with mature [1-^{13}C]F19 Aβ(16−22)E22Q. ^{13}C band positions for antiparallel out-of-register (o) and parallel assemblies (p) are indicated with dashed lines.

Simulations of propagation find that the growing fiber ends can accept strands with altered orientations,[13] and in the aqueous environment on a template where lysine side-chain repulsion may be attenuated and cross-strand pairing to a preorganized glutamine side-chain stabilizing (Figure 3C), conformational "mutations" could accumulate as stabilized by extended glutamine side chain H-bonded Q-tracks. After a certain parallel concentration threshold is reached, fibril fragmentation of mutation-rich domains would generate new parallel ends and grow autocatalytically. This mechanism makes several predictions, which can now be explored through experimentation and simulation. Other mechanistic models, including the glutamine-rich C-termini exposed along the length of the fibril (Figure 5) serving as a secondary nucleation site,[4,5] need also to be explored.

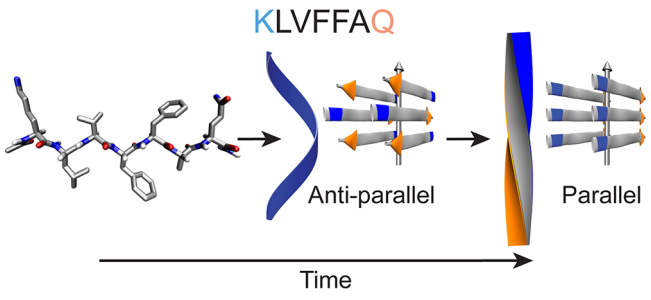

Figure 5. Model for the progressive transitions observed for Aβ(16−22). Paracrystalline forms emerge under these conditions as ribbons with antiparallel out-of-register β-strands. A subsequent transition to fibers is observed with parallel in-register strands. In cartoons, blue represents lysine residues, and orange represents glutamine residues.

Like many materials,[44] these minimal amyloid peptides experience the competing tensions of thermodynamically controlled growth and kinetic nucleation, but amyloid assemblies have also been implicated in disease evolution.[2,45−47] While the larger disease relevant peptides certainly have greater potential for kinetic and thermodynamic conformational diversity, their assembly is also expected to be even more diversified by the complex fluid[48] environment of the eukaryotic cell. The conformational evolution seen in disease likely follows a progressive and irreversible path, and any of these kinetically accessible phases[49] could be nucleated and stabilized by the cellular matrix for a Darwinian-like diversification and selection.[2,45,50] Reconsideration of the confounding determinants required for a conformational evolution in the cell could open new strategies for defining and diverting disease-relevant assemblies for therapeutic intervention.

■ ASSOCIATED CONTENT

Supporting Information

Synthetic and experimental details, including peptide synthesis and purification, synthesis of methylated glutamine, NMR, TEM, CD, and XRD. This material is available free of charge via the Internet at http://pubs.acs.org.

■ AUTHOR INFORMATION

Corresponding Authors

anil.mehta@emory.edu
david.lynn@emory.edu

Present Address

†Department of Developmental Biology, Stanford University School of Medicine, Stanford, CA 94305.

Author Contributions

‡These authors contributed equally.

Notes

The authors declare no competing financial interest.

■ ACKNOWLEDGMENTS

We are indebted to Jeannette Taylor and the Robert P. Apkarian Microscopy Core, Emory University, for TEM training and analyses. The authors acknowledge NSF and NASA Astrobiology Program, under the NSF Center for Chemical Evolution CHE-1004560 for development of peptide congeners and by the Division of Chemical Sciences, Geosciences, and Biosciences, Office of Basic Energy Sciences of the U.S. Department of Energy through Grant DE-ER15377 for structural analyses.

■ REFERENCES

(1) Eichner, T.; Radford, S. E. *Mol. Cell* **2011**, *43*, 8.
(2) Jucker, M.; Walker, L. C. *Nature* **2013**, *501*, 45.
(3) Kabir, M. E.; Safar, J. G. *Prion* **2014**, *8*, 111.
(4) Jeong, J. S.; Ansaloni, A.; Mezzenga, R.; Lashuel, H. A.; Dietler, G. *J. Mol. Biol.* **2013**, *425*, 1765.
(5) Meisl, G.; Yang, X.; Hellstrand, E.; Frohm, B.; Kirkegaard, J. B.; Cohen, S. I. A.; Dobson, C. M.; Linse, S.; Knowles, T. P. J. *Proc. Natl. Acad. Sci. U.S.A.* **2014**, *111*, 9384.
(6) Wood, S. J.; Wetzel, R.; Martin, J. D.; Hurle, M. R. *Biochemistry* **1995**, *34*, 724.
(7) Tjernberg, L. O.; Naslund, J.; Lindqvist, F.; Johansson, J.; Karlstrom, A. R.; Thyberg, J.; Terenius, L.; Nordstedt, C. *J. Biol. Chem.* **1996**, *271*, 8545.

(8) van Duinen, S. G.; Castaño, E. M.; Prelli, F.; Bots, G. T.; Luyendijk, W.; Frangione, B. *Proc. Natl. Acad. Sci. U.S.A.* **1987**, *84*, 5991.
(9) Ma, B.; Nussinov, R. *Proc. Natl. Acad. Sci. U.S.A.* **2002**, *99*, 14126.
(10) Klimov, D. K.; Thirumalai, D. *Structure* **2003**, *11*, 295.
(11) Santini, S.; Mousseau, N.; Derreumaux, P. *J. Am. Chem. Soc.* **2004**, *126*, 11509.
(12) Krone, M. G.; Hua, L.; Soto, P.; Zhou, R.; Berne, B. J.; Shea, J. E. *J. Am. Chem. Soc.* **2008**, *130*, 11066.
(13) Wallace, J. A.; Shen, J. K. *Biochemistry* **2010**, *49*, 5290.
(14) Matthes, D.; Gapsys, V.; de Groot, B. L. *J. Mol. Biol.* **2012**, *421*, 390.
(15) Balbach, J. J.; Ishii, Y.; Antzutkin, O. N.; Leapman, R. D.; Rizzo, N. W.; Dyda, F.; Reed, J.; Tycko, R. *Biochemistry* **2000**, *39*, 13748.
(16) Petty, S. A.; Decatur, S. M. *J. Am. Chem. Soc.* **2005**, *127*, 13488.
(17) Lu, K.; Jacob, J.; Thiyagarajan, P.; Conticello, V. P.; Lynn, D. G. *J. Am. Chem. Soc.* **2003**, *125*, 6391.
(18) Krysmann, M. J.; Castelletto, V.; Hamley, I. W. *Soft Matter* **2007**, *3*, 1401.
(19) Mehta, A. K.; Lu, K.; Childers, W. S.; Liang, Y.; Dublin, S. N.; Dong, J.; Snyder, J. P.; Pingali, S. V.; Thiyagarajan, P.; Lynn, D. G. *J. Am. Chem. Soc.* **2008**, *130*, 9829.
(20) Liang, Y.; Pingali, S. V.; Jogalekar, A. S.; Snyder, J. P.; Thiyagarajan, P.; Lynn, D. G. *Biochemistry* **2008**, *47*, 10018.
(21) Senguen, F. T.; Lee, N. R.; Gu, X.; Ryan, D. M.; Doran, T. M.; Anderson, E. A.; Nilsson, B. L. *Mol. BioSyst.* **2011**, *7*, 486.
(22) Childers, W. S.; Anthony, N. R.; Mehta, A. K.; Berland, K. M.; Lynn, D. G. *Langmuir* **2012**, *28*, 6386.
(23) Liang, Y.; Lynn, D. G.; Berland, K. M. *J. Am. Chem. Soc.* **2010**, *132*, 6306.
(24) Anthony, N. R.; Mehta, A. K.; Lynn, D. G.; Berland, K. M. *Soft Matter* **2014**, *10*, 4162.
(25) Chan, J. C. C.; Oyler, N. A.; Yau, W. M.; Tycko, R. *Biochemistry* **2005**, *44*, 10669.
(26) Schneider, R.; Schumacher, M. C.; Mueller, H.; Nand, D.; Klaukien, V.; Heise, H.; Riedel, D.; Wolf, G.; Behrmann, E.; Raunser, S.; Seidel, R.; Engelhard, M.; Baldus, M. *J. Mol. Biol.* **2011**, *412*, 121.
(27) Bhattacharyya, A. M.; Thakur, A. K.; Wetzel, R. *Proc. Natl. Acad. Sci. U.S.A.* **2005**, *102*, 15400.
(28) Liu, P.; Ni, R.; Mehta, A. K.; Childers, W. S.; Lakdawala, A.; Pingali, S. V.; Thiyagarajan, P.; Lynn, D. G. *J. Am. Chem. Soc.* **2008**, *130*, 16867.
(29) Dong, J.; Shokes, J. E.; Scott, R. A.; Lynn, D. G. *J. Am. Chem. Soc.* **2006**, *128*, 3540.
(30) Brauner, J. W.; Dugan, C.; Mendelsohn, R. *J. Am. Chem. Soc.* **2000**, *122*, 677.
(31) Welch, W. R. W.; Keiderling, T. A.; Kubelka, J. *J. Phys. Chem. B* **2013**, *117*, 10359.
(32) Kubelka, J.; Keiderling, T. A. *J. Am. Chem. Soc.* **2001**, *123*, 6142.
(33) Decatur, S. M. *Acc. Chem. Res.* **2006**, *39*, 169.
(34) Shim, S. H.; Gupta, R.; Ling, Y. L.; Strasfeld, D. B.; Raleigh, D. P.; Zanni, M. T. *Proc. Natl. Acad. Sci. U.S.A.* **2009**, *106*, 6614.
(35) Paul, C.; Axelsen, P. H. *J. Am. Chem. Soc.* **2005**, *127*, 5754.
(36) Petty, S. A.; Decatur, S. M. *Proc. Natl. Acad. Sci. U.S.A.* **2005**, *102*, 14272.
(37) Strasfeld, D. B.; Ling, Y. L.; Gupta, R.; Raleigh, D. P.; Zanni, M. T. *J. Phys. Chem. B* **2009**, *113*, 15679.
(38) Barth, A. *Prog. Biophys. Mol. Biol.* **2000**, *74*, 141.
(39) Jayaraman, M.; Kodali, R.; Sahoo, B.; Thakur, A. K.; Mayasundari, A.; Mishra, R.; Peterson, C. B.; Wetzel, R. *J. Mol. Biol.* **2012**, *415*, 881.
(40) Gregory, D. M.; Mehta, M. A.; Shiels, J. C.; Drobny, G. P. *J. Chem. Phys.* **1997**, *107*, 28.
(41) Gregory, D. M.; Benzinger, T. L.; Burkoth, T. S.; Miller-Auer, H.; Lynn, D. G.; Meredith, S. C.; Botto, R. E. *Solid State Nucl. Magn. Reson.* **1998**, *13*, 149.
(42) Benzinger, T. L. S.; Gregory, D. M.; Burkoth, T. S.; Miller-Auer, H.; Lynn, D. G.; Botto, R. E.; Meredith, S. C. *Proc. Natl. Acad. Sci. U.S.A.* **1998**, *95*, 13407.
(43) Sikorski, P.; Atkins, E. *Biomacromolecules* **2005**, *6*, 425.
(44) Thanh, N. T. K.; Maclean, N.; Mahiddine, S. *Chem. Rev.* **2014**, *114*, 7610.
(45) Li, J.; Browning, S.; Mahal, S. P.; Oelschlegel, A. M.; Weissmann, C. *Science* **2010**, *327*, 869.
(46) Goodwin, J. T.; Mehta, A. K.; Lynn, D. G. *Acc. Chem. Res.* **2012**, *45*, 2189.
(47) Makarava, N.; Baskakov, I. V. *PLoS Pathog.* **2013**, *9*, e1003759.
(48) Fuller, G. G.; Vermant, J. *Annu. Rev. Chem. Biomol. Eng.* **2012**, *3*, 519.
(49) Matsuzaki, K. *Acc. Chem. Res.* **2014**, *47*, 2397.
(50) Collinge, J. *Science* **2010**, *328*, 1111.